Cu K-edge x-ray-absorption spectroscopic study on the octahedrally coordinated trivalent copper in the perovskite-related compounds $La_2Li_{0.5}Cu_{0.5}O_4$ and $LaCuO_3$

Jin-Ho Choy,* Dong-Kuk Kim, and Sung-Ho Hwang
Department of Chemistry, College of Natural Sciences, Seoul National University, Seoul 151-742, Korea

Gérard Demazeau
Laboratoire de Chimie du Solide du CNRS and Interface Hautes Pressions (LCS-CNRS-ENSCPB), Université Bordeaux I, 33405 Talence, Cedex, France

(Received 1 June 1994)

Cu K-edge x-ray-absorption spectra for the chemically well-defined Cu^{III}-containing oxides, $La_2Li_{0.5}Cu_{0.5}O_4$ and $LaCuO_3$, have been carefully studied in order to correlate the complex spectral features with the copper valence, the local symmetry, and the bonding nature. According to the extended x-ray-absorption fine structure spectra, it was found that the (Cu-O) bond distances for both compounds agree well with the x-ray crystallographic data, but in x-ray absorption near-edge structure (XANES) spectra, a clear higher-energy shift of the Cu K-edge position was observed for both trivalent copper oxides compared to divalent ones of Nd_2CuO_4 and La_2CuO_4. When the site symmetry of trivalent copper is lowered from O_h to D_{4h} as in $La_2Li_{0.5}Cu_{0.5}O_4$, the feature by the shakedown process was observed to be split to A and A', corresponding to transitions to the $|1s^13d^{n+1}L^{-1}4p^1_\pi\rangle$ final state and $|1s^13d^{n+1}L^{-1}4p^1_\sigma\rangle$ one, respectively. Therefore, it is proposed that Cu K-edge XANES spectral fine features below the main edge should be interpreted with the molecular-orbital concept, mainly depending upon the copper valence and the crystal-field effect by the local symmetry on the copper site. This work also reveals that a spectral separation ($\sim$2.7 eV) between Cu^{II} and Cu^{III} compounds is smaller than the theoretically expected one ($\sim$4 eV), and the XANES spectrum of metallic compound shows a tendency of a lower energy shift compared to that of insulating or semiconducting one. Thus these facts should be taken into account when determining the presence of trivalent copper from Cu K-edge XANES spectra of copper-based superconductors.

I. INTRODUCTION

After the discovery of copper-based high-T_c superconductors, several studies have been performed to investigate the copper valence, which might be of great importance for understanding the superconducting mechanism, with various analytical techniques such as chemical analysis,[1,2] x-ray photoelectron spectroscopy,[3–8] and x-ray-absorption near-edge structure (XANES) spectroscopy.[9–22] Among them, XANES spectroscopy has been extensively applied to the copper site in the high-T_c superconductors because of its sensitivity to the local electronic and geometrical environments of the proved atom which is stabilized not onto the surface but in the bulk. Cu K-edge XANES spectra reported so far are generally in good agreement with one another, but unfortunately there still exist some controversies with regard to the interpretation of spectral features. Such controversies might be due to two different concepts, molecular orbital (or valence band) (Refs. 9–12 and 23) and multiple scattering (or shape resonance),[13–16] in looking at the same spectral phenomenon.

In the molecular-orbital concept, XANES spectral features correspond to transitions from the Cu 1s core state to the lowest-lying bound states, primarily with p symmetry, and are sensitive to the electronic structure. On the other hand, in a multiple-scattering one, XANES spectral features are due to the interference effects in the final state by multiple scattering of photoelectrons with neighboring atoms mainly depending on the local geometry. However, the two concepts could not be eventually differentiated because the electronic configuration and the local geometry are closely correlated with each other.

In addition, improper reference compounds might also be a source of some controversies in interpreting the Cu K-edge XANES for high-T_c superconducting oxides. Although the compounds such as CuO, $Cu(OH)_2$, and $Cu_2(ac)_4\cdot 2H_2O$ contain only divalent copper ion as Nd_2CuO_4 and La_2CuO_4, Cu K-edge XANES spectral features between two groups are slightly different from each other. Especially, the insulator $ACuO_2$ (A = Na or K) has been frequently used as a reference for the trivalent copper,[17–22] but it seems to be improper for the cuprate superconductors because the electrical properties and geometrical environments around copper in $ACuO_2$ are completely different from those in the copper-based superconductors as pointed out previously.[24] Therefore, a comparison of XANES spectra should be carefully performed with appropriate reference compounds by considering the electrical property as well as local symmetry and crystal structure.

In the present study, we report Cu K-edge XANES and extended x-ray-absorption fine-structure (EXAFS) spec-

tra of the compounds $La_2Li_{0.5}Cu_{0.5}O_4$ and $LaCuO_3$, in which trivalent copper ions are stabilized in a strongly distorted tetragonal site ($c/a = 13.200$ Å/3.731 Å $= 3.54$) and a regular octahedral one, respectively. And it is also difficult to prepare the above Cu^{III} compounds without any oxygen vacancy. Especially, the stoichiometric $LaCuO_3$ oxide can adopt two different structures of tetragonal or rhombohedral form depending on the synthetic condition like oxygen pressure.[25] Therefore, Cu K-edge EXAFS spectra for both compounds were analyzed to identify oxygen stoichiometries and local symmetries around the Cu site, which are important to interpret the present Cu K-edge XANES spectra.

And a comparison of XANES spectra for both compounds with those for the well-known compounds, Nd_2CuO_4 and La_2CuO_4, could allow us to understand more explicitly how the fine structures of Cu K-edge XANES spectrum could be changed with respect to the electronic configurations (Cu^{II} and Cu^{III}), the bonding natures and the bond distances of (Cu-O) bond including the local symmetries. At first, in the electronic structural aspect, Cu K-edge XANES spectra of chemically well-defined $La_2Li_{0.5}Cu_{0.5}O_4$ and $LaCuO_3$ could be a good model for the spectroscopic identification of trivalent copper which is of great interest for the high-T_c cuprate superconductors. And also Cu^{II} compounds of Nd_2CuO_4 and La_2CuO_4 exhibit semiconducting behavior, whereas Cu^{III} compounds of tetragonal $La_2Li_{0.5}Cu_{0.5}O_4$ and rhombohedral $LaCuO_3$ exhibit insulating and metallic conductivity, respectively. Therefore, a comparison of XANES spectra between cuprates showing various conducting properties is surely to be instructive for understanding the spectral fine features in detail. Second, in the structural aspect, Nd_2CuO_4 has the T' structure in which the copper ions are square planarly coordinated with four oxygen ions, where the (Cu-O) bond distance is 1.97 Å.[26] On the other hand, La_2CuO_4 (Ref. 27) and $La_2Li_{0.5}Cu_{0.5}O_4$ (Ref. 28) have the K_2NiF_4-type structure in which the copper ions are tetragonally coordinated with six oxygen ligands, where the equatorial and axial (Cu-O) bond distances are 1.90 and 2.42 Å for the former, and 1.82 and 2.21 Å for the latter, respectively. $LaCuO_3$ has a rhombohedrally distorted perovskite structure, where the copper ions are stabilized in the nearly regular octahedral sites with the (Cu-O) bond distance of 1.94 Å.[28,29] Especially, XANES spectrum on copper having a regular octahedron in solid material has never been known to our knowledge. The K_2NiF_4 structure is closely related to the perovskite structure having the same environment of corner-sharing octahedron around copper site. This similarity of overall crystal structure would approximately make us set aside other factors such as chemical environment beyond the CuO_n ($n = 4$ for Nd_2CuO_4, $n = 6$ for the others) local structure which can influence on the covalency of the (Cu-O) bond and ultimately Cu K-edge XANES spectrum. Now we can consider only the differences of the valences of copper, the (Cu-O) bond distances, and detailed CuO_n local symmetries, which will give us how transitions to bound states and multiple-scattering effect contribute to the fine structures of XANES spectra.

II. EXPERIMENT

A. Sample preparations and characterizations

The Cu^{II} compounds Nd_2CuO_4 and La_2CuO_4 were prepared by conventional solid-state reaction from corresponding binary oxides.[30,31] $La_2Li_{0.5}Cu^{III}{}_{0.5}O_4$ was prepared from the stoichiometric mixture of La_2O_3, CuO, and Li_2O at 870 °C for 28 h under oxygen pressure of 1.6 kbar using a compressed gas apparatus.[28] $LaCu^{III}O_3$ was prepared from the stoichiometric La_2CuO_4 and CuO at 900 °C for 10 min under high oxygen pressure of 60 kbar in order to reduce oxygen vacancy.[28,29] High oxygen pressure was generated *in situ* by thermal decomposition of $KClO_3$, which was already intermixed with reactants before setting in the cell of a belt type high-pressure–high-temperature apparatus.

All compounds were characterized by powder x-ray diffraction (XRD) to check the phase purity. And the crystal structure and the (Cu-O) bond distances for each compound can be seen in Table I, where crystallographic data reported by different authors were used for Nd_2CuO_4 and La_2CuO_4 and those for $La_2Li_{0.5}Cu_{0.5}O_4$ and $LaCuO_3$ were determined by XRD refinement on powder.

Magnetic susceptibility measurements [$\chi_M^{-1} = f(T)$] were carried out using a Faraday-type balance calibrated

TABLE I. Crystallographic data and physical properties of several copper oxides.

Compound	Valence of copper	Crystal structure	(Cu-O) bond distances	Magnetic property	Electric property
Nd_2CuO_4	II	Tetragonal	1.97 Å×4[a]	Antiferromagnetic	Semiconducting
La_2CuO_4	II	Orthorhombic	1.90 Å×4[b]	Antiferromagnetic	Semiconducting
			2.42 Å×2[b]		
$La_2Li_{0.5}Cu_{0.5}O_4$	III	Tetragonal	1.88 Å×4[c]	Diamagnetic	Insulating
			2.23 Å×2[c]		
$LaCuO_3$	III	Rhombohedral	1.94 Å×6[c]	Pauli paramagnetic	Metallic

[a]From Ref. 26.
[b]From Ref. 27.
[c]From Ref. 28.

with $Gd_2(SO_4)_3 \cdot 8H_2O$. Nd_2CuO_4 and La_2CuO_4 show antiferromagnetic properties, whereas $La_2Li_{0.5}Cu_{0.5}O_4$ exhibits diamagnetism representative to trivalent copper in tetragonally distorted octahedron with d^8 low-spin electronic configuration, and $LaCuO_3$ presents Pauli paramagnetism suggesting its metallic character. The conductivity measurements have revealed that Nd_2CuO_4 and La_2CuO_4 show semiconducting behavior, whereas $La_2Li_{0.5}Cu_{0.5}O_4$ and $LaCuO_3$ show insulating and metallic one, respectively.

B. XANES and EXAFS measurements

X-ray-absorption experiments were carried out at the beam line 10B of Photon Factory, National Laboratory for High Energy Physics (KEK-PF), running at 2.5 GeV with a stored current of ~300–360 mA. A Si(311) channel-cut monochromator was used. The resolution was approximately 0.77 eV at the energies of this work. All Cu K-edge x-ray-absorption spectra were recorded in a transmission mode at room temperature. Since the data near the absorption edge must be quite noise-free in order for the second derivative to be useful, the data points are recommended to be closely spaced, i.e., <0.5 eV.[32] Therefore, the data for this work were monitored with a step size of <0.4 eV in the edge region. The samples were prepared in the form of fine powder uniformly dispersed onto the adhesive tape by nujol, which were folded into some layers in order to obtain an edge step, $\Delta\mu t$, of less than 1 and to eliminate pinhole effects as much as possible, both of which contribute to the so-called thickness effect. Energies of the experimental spectra were referenced to the first maximum of the Cu foil calibrant spectrum, defined at 8980.3 eV.

All XANES spectra presented here were normalized by fitting the smooth EXAFS high-energy region with a linear function after subtracting the background extrapolated from the preedge region. And then, the EXAFS oscillations were separated from the absorption background by using a cubic spline background removal technique. Resulting $\chi(k)$ oscillations were weighted with k^3 in order to compensate for the diminishing amplitude of the EXAFS at a high-k region. For analysis of the EXAFS data, a least-squares curve fitting was carried out to the Fourier filtered first coordination shell EXAFS by minimizing the value of F ($F=[\sum k^6(\chi_{\rm cal}-\chi_{\rm expt})^2]^{1/2}/n$, where the summation is performed over the data points (n) in the analyzed k range) with the use of well-known single-scattering EXAFS theory.[33]

III. RESULTS AND DISCUSSION

A. EXAFS analyses

In order to identify whether Cu^{III} compounds of the present study are chemically well defined, the (Cu-O) bond distances and local symmetries around the copper site were investigated by the EXAFS analysis.

Figure 1 shows the Fourier transforms (FT's) of $k^3\chi(k)$ without phase correction from the EXAFS oscillation $\chi(k)$ for Cu^{III} compounds of $LaCuO_3$ and $La_2Li_{0.5}Cu_{0.5}O_4$. The first peak in the FT corresponds to the nearest neighbors of the Cu ion, i.e., a Cu-O shell. This peak was Fourier filtered and backtransformed into the k space for curve-fitting analysis to obtain a quantitative measurement of bond distance between copper and oxygen atoms. The analysis of an EXAFS spectrum requires knowledge of the phase and amplitude functions for a specific absorber-scattering pair. These functions can be calculated theoretically or can be extracted experimentally from the EXAFS spectrum of a structurally well-defined reference compound. In the present study, the phase and amplitude functions derived from the first Cu-O shell of Nd_2CuO_4 were used to analyze the first Cu-O shell of Cu^{III} compounds. In the fitting procedure, only the distance (R) and the Debye-Waller factor (σ^2) were allowed to be refined, but the coordination number (N) was fixed to a reasonable integer because of the inaccuracies in refined N values caused by strong correlation with σ^2. Quantitative results from nonlinear least-squares fitting for the Fourier-filtered first coordination shell are presented in Table II and Fig. 2. From the EXAFS result for $LaCuO_3$, the CuO_6 octahedron is found to be nearly regular with a (Cu-O) bond distance of 1.94(6) Å in all crystallographic axes, which is in good agreement with that by neutron-diffraction refinement [1.9511(3) Å] (Ref. 34) or by x-ray-diffraction refinement [1.94(3) Å].[28,29] But curve fitting for the Fourier-filtered first coordination shell of $La_2Li_{0.5}Cu_{0.5}O_4$ could not be successfully achieved with a single-shell model of six oxygen atoms, as expected from the K_2NiF_4-type structure. Therefore a two-shell model should be employed in fitting the Cu-O shell, which produced much better result: four

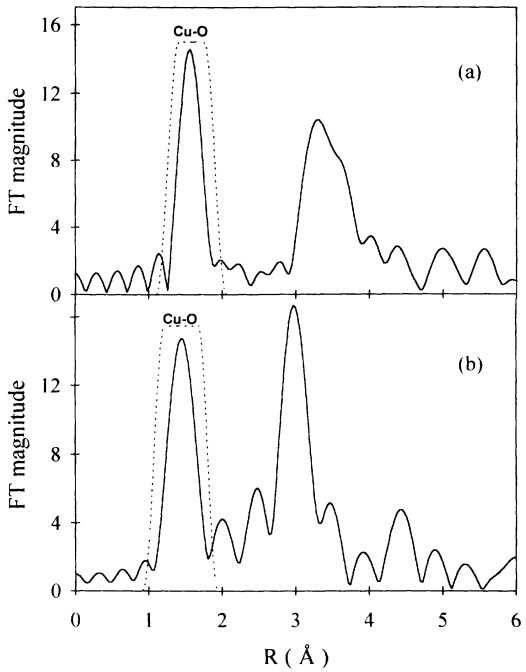

FIG. 1. Fourier transforms of k^3-weighted Cu K-edge EXAFS for (a) $LaCuO_3$ and (b) $La_2Li_{0.5}Cu_{0.5}O_4$, along with the filtering windows (dashed curves). The first peak corresponds to the Cu-O shell.

TABLE II. Structural parameters obtained from EXAFS analysis using Nd_2CuO_4 as a reference.

Compound	Bonding	$\Delta R_{\text{filtered}}$ (Å)[a]	Δk (Å^{-1})[b]	N[c]	R (Å)	$10^3\Delta\sigma^2$ (Å^2)[d]	F[e]
$LaCuO_3$	Cu-O	1.32–1.89	2.3–13.5	6	1.94(6)	−0.04	0.06
$La_2Li_{0.5}Cu_{0.5}O_4$	$Cu-O_{eq}$	1.24–1.79	3.0–13.5	4	1.82(4)	−2.30	0.53
	$Cu-O_{ax}$			2	2.21(8)	+0.60	

[a]Range of back-Fourier transform.
[b]Range of least-squares curve fitting.
[c]Fixed at values during fitting.
[d]The variation of the Debye-Waller factor relative to that of a reference.
[e]$F=[\sum k^2(\chi_{\text{cal}}-\chi_{\text{expt}})^2]^{1/2}/n$, where n is the number of data point.

equatorial (Cu-O) bond distances of 1.82(4) and two axial ones of 2.21(8) Å. Direct comparison with the diffraction data was not possible for $La_2Li_{0.5}Cu_{0.5}O_4$ due to the absence of definitive crystallographic data for the oxygen positions in this system. But this result is very reliable when it is compared with the previously characterized K_2NiF_4-type compound, $SrLaCu^{III}O_4$,[35] in which the equatorial and axial (Cu-O) bond distances are 1.88 and 2.23 Å, respectively. The axial (Cu-O) bond distances of both compounds are similar, whereas the equatorial one in $La_2Li_{0.5}Cu_{0.5}O_4$ is much smaller than that in $SrLaCuO_4$, despite the trivalent copper with the isotype-tetragonally distorted local symmetry in both compounds. This fact might result from the enhanced covalency of the (Cu-O) bond due to the weaker competing (Li-O) bond along the equatorial bond sequence of (-O-Cu-O-Li-O-) in the system of $La_2Li_{0.5}Cu_{0.5}O_4$, compared to the case of $SrLaCuO_4$. The Debye-Waller factor (σ^2) in the EXAFS function means the mean-square deviation in the average distance between absorbing and scattering pair, and reflects thermal (σ^2_{vib}) and static distortions (σ^2_{sta}) due to thermal and structural variations within a shell, respectively. It is clearly seen in Table II that the Debye-Waller factors relative to that of a reference, Nd_2CuO_4, well correlate with the bond distances. This fact indicates that there are little static distortions in (Cu-O) bonds of Cu^{III} compounds.

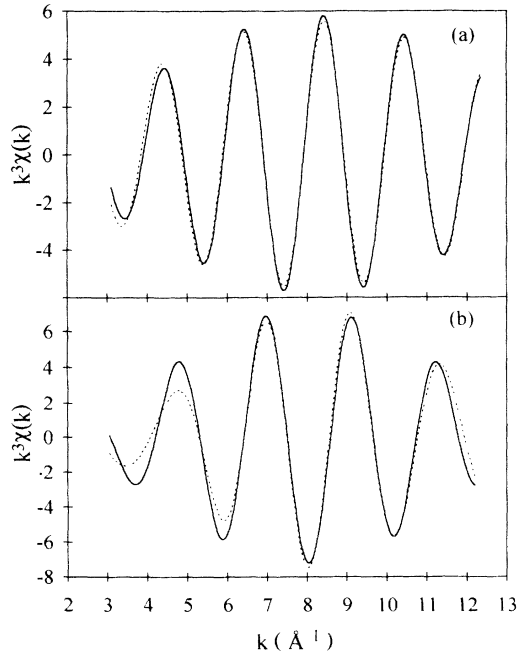

FIG. 2. Fourier-filtered experimental EXAFS for the first peak (——) and the least-squares best fits (· · · ·) for (a) $LaCuO_3$, and (b) $La_2Li_{0.5}Cu_{0.5}O_4$.

B. XANES analyses

Normalized Cu K-edge XANES spectra of Nd_2CuO_4, La_2CuO_4, $La_2Li_{0.5}Cu_{0.5}O_4$, and $LaCuO_3$ are shown in Fig. 3, where the zero of energy was chosen to be the first peak position of the Cu foil edge spectrum (8980.3 eV). As expected, there is a significant shift of the edge position between the divalent compounds and the trivalent ones. Such an observation is in good agreement with a general expectation that the core level becomes more tightly bound with an increase of valence, which results in an increase of transition energy from the 1s to the final states, even though further detailed identification on spectral fine features must be followed. Though the Cu K-edge XANES spectrum of $LaCuO_3$ was already reported,[36] the existence of trivalent copper was ruled out by comparing the XANES spectra of various compounds containing divalent copper ion such as $Cu(NH_3)_4SO_4$, La_2CuO_4, and $YBa_2Cu_3O_{7-y}$. However, their conclusion might be somewhat ambiguous because in interpreting the spectral fine features, local symmetry around copper was not taken into account. Moreover, it seems to be problematic in energy calibration in comparing the XANES spectra for La_2CuO_4 and $YBa_2Cu_3O_{7-y}$ previously reported by other groups.

In Fig. 4, the corresponding second derivative curves are present in order to identify the fine features in the edge region and to locate them more accurately in energy. And the position of each peak in Table III was obtained from the first derivative curves as well as the second derivative ones.

1. *Preedge feature*

All the spectra show a preedge feature denoted as P corresponding to transition from the 1s core level to the final states with unoccupied 3d states. The position of this feature for $La_2Li_{0.5}Cu_{0.5}O_4$ (− 2.2 eV) and $LaCuO_3$ (−2.2 eV) is about 1 eV higher than that for Nd_2CuO_4 (−3.3 eV) and La_2CuO_4 (−3.4 eV). Such an increase in energy supports the existence of trivalent copper in

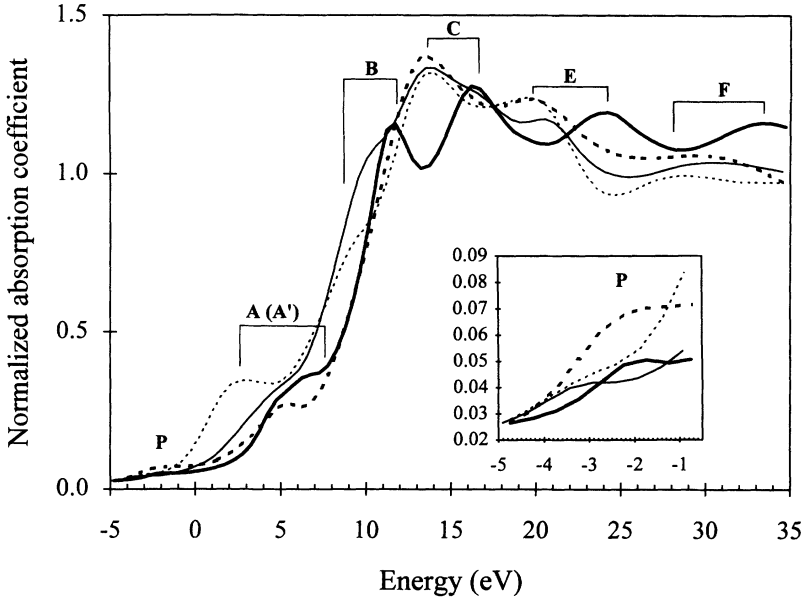

FIG. 3. Comparison of Cu K-edge XANES spectra for $LaCu^{III}O_3$ (— — —), $La_2Li_{0.5}Cu^{III}_{0.5}O_4$ (——), $La_2Cu^{II}O_4$ (——), and $Nd_2Cu^{II}O_4$ (· · · ·). The inset shows the enlarged-scale view of preedge feature.

$La_2Li_{0.5}Cu_{0.5}O_4$ and $LaCuO_3$. Since the present compounds have an inversion symmetry around the copper site, this preedge feature is primarily forbidden by electric dipole selection rule, $\Delta l = \pm 1$, but it might be mainly attributed to a quadrupole-allowed transition.[37] Thus the intensity of this feature is associated with the $3d$ hole density in the ground state, resulting in high intensities for Cu^{III} compounds, $La_2Li_{0.5}Cu_{0.5}O_4$ and $LaCuO_3$ as can be clearly seen in Figs. 3 and 4. But this feature appears to be higher in intensity for $LaCuO_3$ than that for $La_2Li_{0.5}Cu_{0.5}O_4$ even though both have the same trivalent copper in the lattice, which might result from the partially dipole allowed transition by mixing of p character into the d state due to a certain delocalization of d electrons in $LaCuO_3$ showing metallic property, contrary to insulating $La_2Li_{0.5}Cu_{0.5}O_4$.

2. *Main-edge features*

The other peaks denoted as A (or A'), B, and C in Figs. 3 and 4 are related to the dipole-allowed transition from the $1s$ core to the $4p$ states core states in molecular orbital concept.[10–12,23,38–40] But, on the other hand, such edge structures are explained in terms of the multiple-scattering effects by many previous works on multiple scattering one-electron calculations, which depend mainly on the geometrical structure rather than the electronic one.[13–16,41] But multiple-scattering calculations performed to date have generally not achieved much better than qualitative agreement with experiment because of the intrinsic limitations of the present muffin-tin approximation of the potential. Therefore, it is interesting to examine the relationship between crystal structure and spectral feature of Nd_2CuO_4 and La_2CuO_4 in order to certify qualitatively the influence of the multiple-scattering effect upon the XANES. As shown in Table I, the (Cu-O) bond distances for Nd_2CuO_4 are very different from those for La_2CuO_4. Moreover, there is little similarity in our calculation on the possible multiple-scattering paths for the six-shell model clusters of $CuO_4Nd_8O_8Cu_4Nd_2O_8$ for Nd_2CuO_4 and $CuO_4O_2La_8Cu_4O_8O_8$ for La_2CuO_4, respectively, as expected. As shown in Figs. 3 and 4, both spectra, however, exhibit almost the same peak positions and similar spectral fine features except for peak A. In addition, a

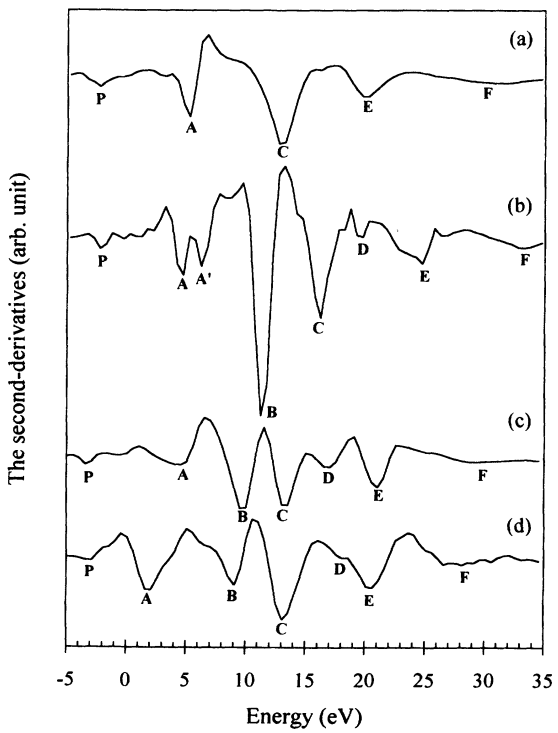

FIG. 4. The second-derivative curves of Cu K-edge XANES spectra for (a) $LaCu^{III}O_3$, (b) $La_2Li_{0.5}Cu^{III}_{0.5}O_4$, (c) $La_2Cu^{II}O_4$, and (d) $Nd_2Cu^{II}O_4$.

TABLE III. Energies of Cu K-edge spectral features for several copper oxides given in Figs. 3 and 4. All energies are referenced to the first maximum of Cu foil, 8980.3 eV. Measurements are in units of eV.

Compound	P	A	A'	B	C	D	E	F
Nd_2CuO_4	−3.3	3.1		9.1	13.4	17.3	20.6	28.8
La_2CuO_4	−3.4	4.6		9.6	13.3	17.1	20.6	30.7
$La_2Li_{0.5}Cu_{0.5}O_4$	−2.2	4.8	6.3	11.5	16.3	19.5	24.5	33.5
$LaCuO_3$	−2.2	5.3			13.3		19.8	29.5

large ratio (d_a/d_e) of the axial distances (d_a) versus the equatorial ones (d_e) between copper and oxygen in the tetragonally distorted symmetry has caused a larger splitting of peaks B and C, according to the multiple-scattering calculations.[15] But in the comparison of La_2CuO_4 and $La_2Li_{0.5}Cu_{0.5}O_4$, they do not agree well with this expectation even though they have the same K_2NiF_4 structure, since La_2CuO_4 with a larger ratio of d_a/d_e (=1.274) exhibits even a smaller splitting of 3.7 eV rather than 4.8 eV for $La_2Li_{0.5}Cu_{0.5}O_4$ (d_a/d_e=1.216). Of course, it is clear that our spectral features are also affected by the local symmetries around the copper site as expected in the multiple-scattering calculations. That is, there is no splitting of the main peak (C) in $LaCuO_3$ with a nearly regular octahedron of CuO_6, whereas there are splittings of peaks B and C in Nd_2CuO_4, La_2CuO_4 and $La_2Li_{0.5}Cu_{0.5}O_4$ with a square planar or a tetragonally distorted octahedron.

However, these spectral features could be well explained with the molecular orbitals concept considering both of the electronic configuration and the local symmetry on the copper site. Kosugi *et al.*[10] suggested through the polarized XANES studies that Cu K-edge spectra for the compounds with the local symmetries of square planar or tetragonally distorted octahedron could be separated into two regions corresponding to the $1s \rightarrow 4p_\pi$ (in-plane) and the $1s \rightarrow 4p_\sigma$ (out-of-plane) transitions and each transition shows twin-peak structures, in which the lower-energy peak corresponds to the transition to well-screened core-hole final state involving a shakedown process by ligand-to-metal-charge transfer (LMCT) and the higher-energy peak to the transition to poorly screened one. According to these interpretations for the present study, the fine features A, B, C, and E in Figs. 3 and 4 could be assigned as the transition to the core-hole final state of $|1s^1 3d^{n+1} L^{-1} 4p_\pi^1\rangle$, $|1s^1 3d^n 4p_\pi^1\rangle$, $|1s^1 3d^{n+1} L^{-1} 4p_\sigma^1\rangle$, and $|1s^1 3d^n 4p_\sigma^1\rangle$, respectively, where L^{-1} denotes a ligand hole. But such assignments seem to be incorrect because the presence of feature E in $LaCuO_3$ and the splitting of feature A in $La_2Li_{0.5}Cu_{0.5}O_4$ cannot be well explained in this way, which will be thoroughly discussed later. On the other hand, Dartyge *et al.*[11] have argued against the above interpretation in the study on anisotropy of shakedown process by comparing the polarized XANES spectra for both La_2CuO_4 and Pr_2NiO_4, those of which have K_2NiF_4 structure with almost the same (Cu/Ni-O) bond distances. In their study, the Ni K-edge polarized XANES spectrum for Pr_2NiO_4 was different from the Cu K-edge one for La_2CuO_4, showing the weak intensities of the poorly screened transitions (D and E) for Pr_2NiO_4, and such differences were thought to be due to a shakedown process occurring through only one channel ($d_{x^2-y^2}$) in cuprate but two quasiequivalent channels ($d_{x^2-y^2}$ and d_{z^2}) in nickelate. Therefore, they concluded that peak A is due to the geometrical structure by the farther neighbors and B, C, D, and E are originated from transition to the final state of $|1s^1 3d^{n+1} L^{-1} 4p_\pi^1\rangle$, $|1s^1 3d^n 4p_\pi^1\rangle$, $|1s^1 3d^{n+1} L^{-1} 4p_\sigma^1\rangle$, and $|1s^1 3d^n 4p_\sigma^1\rangle$, respectively. But the Cu K-edge XANES spectrum for $La_2Li_{0.5}Cu_{0.5}O_4$ in this study exhibits well-defined features of A, B, C, D, and E contrary to the Ni K-edge one for Pr_2NiO_4, even though copper and nickel for each compound have the same electronic configuration of d^8 as well as the structural similarity including metal oxygen bond distances. These facts imply that their interpretation may not be generally applicable, and divalent nickel also cannot represent the characteristics of trivalent copper.

It becomes clear now why Cu K-edge XANES spectra for the chemically well-defined Cu^{III} compounds cannot be well explained with the early proposed interpretations. Therefore, a modification of such previous interpretations should be made to explain the spectral fine features above the edge ramp in the present Cu K-edge XANES spectra. Peak A for Nd_2CuO_4 and La_2CuO_4 in Figs. 3, 4(a), and 4(b) has been generally accepted as a transition to the $4p_\pi$ state accompanied by a shakedown process through charge transfer from the ligands to the Cu $3d$ hole, which enhances the screening of the core hole resulting in lower transition energy.[23] And the position and intensity of this peak are determined by the local symmetry on the copper site and the valence state. As shown in Figs. 3, 4(a), and 4(b) for the cases of Nd_2CuO_4 and La_2CuO_4, it has been theoretically and experimentally understood that the shakedown process by the ligand-to-metal-charge transfer is effectively reduced by the presence of apical oxygens and vanishes when the local symmetry around copper is almost cubic, which results in the electrostatic repulsion against the attractive potential created by the core hole.[42] Therefore, it is at first expected that peak A due to the shakedown process for $LaCuO_3$ may not be observed only by considering it with the geometrical point of view. But in the actual spectrum of Figs. 3 and 4(d), this peak could be observed with a prominent intensity at higher energy than that of Cu^{II} compounds. This phenomenon supports the increase of copper valence, which electrostatically favors the charge transfer from oxygen ligand to copper, irrespective of the pres-

ence of the apical oxygens. Moreover, $La_2Li_{0.5}Cu_{0.5}O_4$ exhibits the splitting (A and A') of the feature by the shakedown process, which becomes more significant in the second-derivative curve of Fig. 4(c). And the split A and A' peaks might correspond to the transitions to the $|1s^1 3d^{n+1}L^{-1}4p_\pi^1\rangle$ final state and the $|1s^1 3d^{n+1}L^{-1}4p_\sigma^1\rangle$ one, respectively, through both π- and σ-bonding channels resulting from the electrostatically enhanced attractive potential of trivalent copper, as already suggested for the trivalent copper compound, $LaCuO_3$. The possibility that the shakedown process along the σ bonding will be present at lower energy than the poorly screened core-hole $4p_\pi$ final state, if any, can be supported by the origins of the higher-energy features to be discussed in the following. Besides the assignments of spectral fine features based on multiple-scattering calculation or molecular orbitals as mentioned above, a number of researchers have assigned the peaks B and C to $1s \rightarrow 4p_\pi$ and $1s \rightarrow 4p_\sigma$ transitions, respectively, without discussing on the local symmetry of copper, even though such an assignment is not surprising when the tetragonally distorted CuO_6 in K_2NiF_4 structure is taken into account. But $LaCuO_3$ could give a clear answer for these assignments because the copper $4p$ orbitals are isotropic in this system. It is therefore expected that only one transition of $1s \rightarrow 4p_\sigma$ might be available for the isotropic CuO_6. Such an assumption becomes true if we observe only peak C in Figs. 3 and 4(d). Now there is no more bound state with p character in $LaCuO_3$. Therefore, peak E in $LaCuO_3$ could not be attributed to the transition to the poorly screened $4p_\sigma$ state which Kosugi *et al.*[10] and Dartyge *et al.*[11] have assigned. On the other hand, the degeneracy of the copper $4p$ state in Nd_2CuO_4 and La_2CuO_4 will be lifted into $4p_\pi(a_{2u})$ and $4p_\sigma(e_u)$ states by an anisotropic crystal-field effect on the copper site. The features B and C in Figs. 3, 4(a), and 4(b) correspond to the transition to the $|1s^1 3d^9 4p_\pi^1\rangle$ and the $|1s^1 3d^9 4p_\sigma^1\rangle$ final states, respectively, and peak E should be attributed to the same origin as $LaCuO_3$. It should be noted that the position (13.3 eV) of feature C in $LaCuO_3$ is nearly the same as that of Nd_2CuO_4 (13.4 eV) or La_2CuO_4 (13.3 eV), but this similarity is only fortuitous. If the copper is divalent in $LaCuO_3$ with the local symmetry of regular octahedron as Webb *et al.*[36] argued in the previous XANES study, peak C in $LaCuO_3$ must be positioned between B and C in Nd_2CuO_4 or La_2CuO_4 with the local symmetry of square planar or tetragonally distorted octahedron, respectively. But the copper in $LaCuO_3$ is trivalent, so that the Cu $4p$ orbitals are degenerated whose energy levels are almost identical with those of $4p_\sigma$ for Cu^{II} as shown in Fig. 5.

$La_2Li_{0.5}Cu_{0.5}O_4$ can also support our assignments of peaks B and C, which are present at higher energies than those of Nd_2CuO_4 and La_2CuO_4, reflecting the increase of copper valence. Moreover, more prominent intensities and further split of both features compared to those of Nd_2CuO_4 and La_2CuO_4 represent the enhanced crystal-field effect as generally expected in the high valent metal compounds.

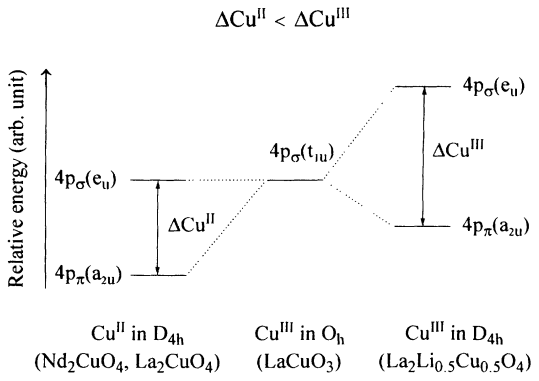

FIG. 5. Energy level diagram of $4p$ final states relative to $1s$ core-hole state for a CuO_6 octahedron. In D_{4h} symmetry, crystal-field splitting (ΔCu^{III}) for the trivalent copper is stronger than that (ΔCu^{II}) for the divalent one.

3. *Post-edge features*

Unlike lower-energy features, however, higher-energy ones of D, E, and especially F are not significantly dependent on the valence state of copper as shown in Table III, and such phenomena have been generally explained by the multiple-scattering effect, even though peak D has been little noticed because of its low intensity. But Guo *et al.* have pointed out that D and E might be due to the shakeup processes involving the Cu $3d \rightarrow 4p$ transitions in the core-hole final states through the theoretical XANES studies for La_2CuO_4 (Ref. 43) and $YBa_2Cu_3O_{7-\delta}$.[44] According to their expectation, $LaCuO_3$ must have only one shakeup process because of its isotropic bonding nature on the copper site. In fact, the present spectrum $LaCuO_3$ shows only one peak, E and the energy differences between D and E for Nd_2CuO_4, La_2CuO_4, and $La_2Li_{0.5}Cu_{0.5}O_4$ with the D_{4h} symmetry are 3.3 3.5, and 5 eV, respectively, which shows a strong dependency in the copper valence. From the fact that our experimental data are in good agreement with the theoretical expectation, these features should result from the shakeup processes, even though features above E include a considerable multiple scattering.

4. *Copper valence and edge shift*

It should be noted that although spectra for $La_2Li_{0.5}Cu_{0.5}O_4$ and $LaCuO_3$ entirely shift to the higher energies compared to those for Nd_2CuO_4 and La_2CuO_4, representing the increase of copper valence, the degree of shift of each feature is different from each other. That is, main edge jumps above A for $La_2Li_{0.5}Cu_{0.5}O_4$ and La_2CuO_4 are separated by 1.8 eV, whereas shifts of B and C are 1.9 and 3 eV, respectively. From these facts, it is clear that valence state assignments, based on the position of main edge jump frequently used by many authors, are problematic since each molecular-orbital state experiences the crystal-field effect differently by the evolution of valence state. However, to our knowledge, an empirical

rule for the relationship between the valence of $3d$ transition-metal ions including Cu and the overall K-edge spectral features has not been established, even though there has been an attempt to take into account the overall edge features for determining the copper valence.[45] Therefore, it is proposed that the centroid position between B and C could be correlated with the copper valence state. In the present study, the centroid positions between B and C for Cu^{II} compounds of Nd_2CuO_4 and La_2CuO_4 show almost the same value of 11.97 and 12.07 eV, respectively, whereas $La_2Li_{0.5}Cu_{0.5}O_4$ shows higher value of 14.07 eV compared to 13.3 eV for $LaCuO_3$. Such a discrepancy might be associated with their different natures of electron localization and delocalization as can be seen from the insulating and metallic properties for $La_2Li_{0.5}Cu_{0.5}O_4$ and $LaCuO_3$, respectively. In fact, the copper valence in metallic $LaCuO_3$ might be somewhat less than trivalent because of the strong hybridization between copper and oxygen in metallic $LaCuO_3$, as previously reported in the band-structure calculation for this system.[29,46] On the other hand, the bond in insulating $La_2Li_{0.5}Cu_{0.5}O_4$ is less covalent than $LaCuO_3$, which was also confirmed by its diamagnetism. Such a relation between electrical property and edge energy is well consistent with the previous Fe K-edge study for various iron oxides.[47] Therefore, the tendency of a lower-energy shift of the metallic compound compared to an insulating or semiconducting one should be considered in determining the metal valence from XANES spectra.

Moreover, a spectral separation between Cu^{III} and Cu^{II} is ~ 2.7 eV when comparing the centroid positions of $La_2Li_{0.5}Cu_{0.5}O_4$ (14.7 eV) and Nd_2CuO_4 (11.97 eV) or La_2CuO_4 (12.07 eV). Though this value is less than the theoretically expected one, ~ 4 eV,[17] it is noteworthy here that it is the value obtained experimentally for the first time from the chemically well-defined Cu^{II} and Cu^{III} systems.

IV. CONCLUSION

XANES spectral fine features below the main peak, C, could be well assigned to the transitions from an initial $1s$ core state to bound molecular orbitals, which are mainly dependent on the valence state of copper and the crystal field associated with the local symmetry, not on the bond distances. Even though a contribution of multiple scattering cannot be completely ruled out for lower-energy features, our systematic experiment clearly indicates that the change of spectral fine features cannot be effectively explained only by the multiple-scattering concept. In determining the presence of trivalent copper from Cu K-edge XANES spectra of copper-based superconductors, its metallic property at room temperature and the small separation of ~ 2.7 eV between Cu^{II} and Cu^{III} as well as the change of bonding nature due to the partial presence of Cu^{III} should be taken into account. But the position of feature A corresponding to the transition to the well-screened final state with a shakedown process can be a good standard for determining the copper valence since it is nearly constant irrespective of the local symmetry on the copper site for Cu^{III} compounds. On the other hand, it depends rather significantly on the local symmetry in the case of Cu^{II} ones.

In conclusion, chemically well-defined Cu^{III} compounds, $La_2Li_{0.5}Cu_{0.5}O_4$ and $LaCuO_3$ could enable us to estimate the valence and local symmetry contributions to the complicated XANES of copper-oxide materials.

ACKNOWLEDGMENTS

We thank the Photon Factory, National Laboratory for High Energy Physics (Proposal No. 92G196) and the Pohang Light Source (Proposal No. 92-012) for supporting the synchrotron radiation experiments. We are very grateful to Professor M. Nomura for his help in x-ray-absorption experiments at the beamline BL 10B, and also to the KOSEF (92-25-00-02) and CNRS for the support of the high-pressure experiments (1993). Our thanks are extended to the Korean Ministry of Science and Technology (MOST) for the high-T_c superconductivity research fund (1993–1994).

*Author to whom all correspondence should be addressed. Electronic address: jhchoy@ibm3090.snu.ac.kr

[1] J. Norvak, P. Vyhlidka, D. Zemanova, E. Pollert, and A. Triska, Physica C **157**, 346 (1989).
[2] S. X. Dou, H. K. Liu, A. J. Bourdillon, N. Savvides, J. P. Zhou, and C. C. Sorrell, Solid State Commun. **68**, 221 (1988).
[3] J. H. Choy, D. Y. Jung, and Q. W. Choi, Mol. Cryst. Liq. Cryst. **184**, 61 (1990).
[4] J. H. Choy, W. Y. Choe, and D. Y. Jung, J. Phys. Chem. Solids **52**, 545 (1991).
[5] J. C. Park, S. G. Kang, J. H. Choy, A. Wattiaux, and J. C. Grenier, Physica C **185-189**, 567 (1991).
[6] J. H. Choy, D. Y. Jung, S. J. Kim, Q. W. Choi, and G. Demazeau, Physica C **185-189**, 763 (1991).
[7] A. Balzarott, M. De Crescenzi, N. Motta, F. Patella, and A. Sgarlata, Phys. Rev. B **38**, 6461 (1988).
[8] E. Sacher and J. E. Klemberg-Sapieha, Phys. Rev. B **39**, 1461 (1989).
[9] H. Oyanagi, H. Ihara, T. Matsubara, M. Tokumoto, T. Matsushita, M. Hirabayashi, K. Murata, N. Terada, T. Yao, H. Iwasaki, and Y. Kimura, Jpn. J. Appl. Phys. **26**, L1561 (1987).
[10] N. Kosugi, H. Kondoh, H. Tajima, and H. Kuroda, Chem. Phys. **135**, 149 (1989).
[11] D. Dartagy, A. Fontaine, F. Baudelet, C. Giorgetti, S. Pizzini, and H. Tolentino, J. Phys. (France) I **2**, 1233 (1992).
[12] G. Liang, A. Sahiner, M. Croft, W. Xu, X. D. Xiang, D. Badresingh, W. Lu, J. Chen, J. Peng, A. Zettl, and F. Lu, Phys. Rev. B **47**, 1029 (1993).
[13] F. W. Lytle and R. B. Greegor, Phys. Rev. B **37**, 1550 (1988).
[14] K. B. Gard, A. Bianconi, S. D. Longa, A. Clozza, and M. De Santis, Phys. Rev. B **38**, 244 (1988).

[15]J. Garcia, M. Benfatto, C. R. Natoli, A. Bianconi, A. Fontaine, and H. Tolentino, Chem. Phys. **132**, 295 (1989).
[16]A. Bianconi, C. Li, F. Campanella, S. D. Longa, I. Pettiti, M. Pompa, S. Turtù, and D. Udron, Phys. Rev. B **44**, 4560 (1991).
[17]F. Baudelet, G. Collin, E. Dartagy, A. Fontaine, J. P. Kappler, G. Krill, J. P. Itie, J. Jegoudez, M. Maurer, Ph. Monod, A. Revcolevschi, H. Tolentino, G. Tourillon, and M. Verdaguer, Z. Phys. B **69**, 141 (1987).
[18]J. M. Tranquada, S. M. Heald, and A. R. Moodenbaugh, Phys. Rev. B **36**, 5263 (1987).
[19]J. B. Boyce, F. Bridges, T. Claeson, R. H. Howland, and T. H. Geballe, Phys. Rev. B **36**, 5251 (1987).
[20]E. E. Alp, G. K. Shenoy, D. G. Hinks, D. W. Capone II, L. Soderholm, H. B. Schuttler, J. Guo, D. E. Ellis, P. A. Montano, and R. Ramanathan, Phys. Rev. B **35**, 7199 (1987).
[21]B. Lengeler, M. Wilhelm, B. Jobst, W. Schwaen, B. Seebacher, and U. Hillebrecht, Solid State Commun. **65**, 1545 (1988).
[22]R. Retoux, F. Studer, C. Michel, B. Raveau, A. Fontaine, and E. Dartyge, Phys. Rev. B **41**, 193 (1990).
[23]R. A. Bair and W. A. Goddard III, Phys. Rev. B **22**, 2767 (1980).
[24]K. Allan, A. Campion, J. Zhou, and J. B. Goodenough, Phys. Rev. B **41**, 11 572 (1990).
[25]S. Darracq, A. Largeteau, G. Denazeau, B. A. Scott, and J. F. Bringley, Eur. J. Solid State Inorg. Chem. **t29**, 585 (1992).
[26]T. Kajitani, K. Hirage, S. Hosoya, T. Fukuda, K. Oh-Ishi, M. Kikuchi, Y. Syono, S. Tomiyoshi, M. Takahashi, and Y. Muto, Physica C **169**, 227 (1990).
[27]P. Zolliker, D. E. Cox, J. B. Parise, E. M. McCarron III, and W. E. Farneth, Phys. Rev. B **42**, 6332 (1990).
[28]G. Demazeau, C. Parent, M. Pouchard, and P. Hagenmuller, Mater. Res. Bull. **7**, 913 (1972).
[29]S. Darracq, S. Matar, and G. Demazeau, Solid State Commun. **85**, 961 (1993).
[30]Y. Tokura, H. Takagi, and S. Uchida, Nature **337**, 345 (1989).
[31]A. N. Christensen, Acta Chem. Scand. **44**, 769 (1990).
[32]F. W. Lytle and R. B. Greegor, Appl. Phys. Lett. **56**, 192 (1990).
[33]B. K. Teo, *EXAFS: Basic Principles and Data Analysis* (Springer-Verlag, New York, 1986).
[34]D. B. Currie and M. T. Weller, Acta Crystallogr. C **47**, 696 (1991).
[35]J. B. Goodenough, G. Demazeau, M. Pouchard, and P. Hagenmuller, J. Solid State Chem. **8**, 325 (1973).
[36]A. W. Webb, K. H. Kim, and C. Bouldin, Solid State Commun. **79**, 507 (1991).
[37]J. E. Hahn, R. A. Scott, K. O. Hodgson, S. Doniach, S. R. Desjardins, and E. I. Solomon, Chem. Phys. Lett. **88**, 595 (1982).
[38]L. A. Grunes, R. D. Leapman, C. N. Willker, R. Hoffmann, and A. B. Kunz, Phys. Rev. B **25**, 7157 (1982).
[39]N. Kosugi, T. Yokyama, K. Asakura, and H. Kuroda, Chem. Phys. **91**, 249 (1984).
[40]T. Yokoyama, N. Kosugi, and H. Kurada, Chem. Phys. **103**, 101 (1986).
[41]T. A. Smith, J. E. Penner-Hahn, M. A. Berding, S. Doniach, and K. O. Hodgson, J. Am. Chem. Soc. **107**, 5945 (1985).
[42]J. M. Tranquada, S. M. Heald, A. R. Moodenbaugh, G. Liang, and M. Croft, Nature (London) **337**, 720 (1989).
[43]J. Guo, D. E. Ellis, G. L. Goodman, E. E. Alp, L. Soderholm, and G. K. Shenoy, Phys. Rev. B **41**, 82 (1990).
[44]J. Guo, D. E. Ellis, E. E. Alp, and G. L. Goodman, Phys. Rev. B **42**, 251 (1990).
[45]E. E. Alp, G. L. Goodman, L. Soderholm, S. M. Mini, M. Ramanathan, G. K. Shenoy, and A. S. Bommannavar, J. Phys.: Condens. Matter **1**, 6463 (1989).
[46]K. Takegahara, Jpn. J. Appl. Phys. **26**, L437 (1987).
[47]B. Buffat, M. H. Tuilier, H. Dexpert, G. Demazeau, and P. Hagenmuller, J. Phys. Chem. Solids **47**, 491 (1986).